Inner Surface Modification of Tube Materials by Grid-Enhanced Plasma Source Ion Implantation Method

Zhang Gu-Ling, Wang Jiu-Li, Fan Song-Hua, Liu Yuan-Fu, Liu Chi-Zi, Yang Si-Ze

Institute of Physics, Chinese Academy of Science, Beijing, China 100080
Email: glzhang@aphy.iphy.ac.cn Tel: 86-10-82649458

Abstract – Inner surface coating of tubular sample was realized by a new method of grid-enhanced plasma source ion implantation (GEPSII). In GEPSII, an radio frequency (rf) plasma core is produced between a central cathode and a grid electrode, which are coaxially arranged inside the tubular sample. Negative high voltage applied between the grid electrode and the inner surface of the tubular sample for implantation. And the implantation can greatly improve the surface anticorrosion ability of 0.45% C steel sample (45# steel). But we found shadow effect in our experiments. To reduce the shadow effect and obtain accordingly better implantation uniformity of sample surfaces, lower implanting voltage, higher gas pressure and smaller grid radius are needed. And an axial magnetic field can increase the plasma density inside the tube and mix the plasma outside the grid, so the shadow effect of sample surfaces will be weakened.

1. Introduction

Plasma source ion implantation (PSII) or plasma immersion ion implantation (PIII) is a relatively new technique for material fabrication and surface treatment [1, 2]. Its nonline-of-sight advantage makes it a superior technique for enhancing the properties and performance of large or irregular shaped work-pieces [3, 4]. In PSII, it is easy to implant the naked parts of a working piece, but difficult to implant the inner surface of components such as a gun-barrel, a cylinder of automobile or an oil delivery pipe. In recent years, PSII for inner surface modification has aroused great interests of plasma scientists and engineers, and some experiments have been developed to improve the inner surface properties of tubes [5–9]. But bad uniformity and film firmness are two chief obstacle thus far unresolved. We have recently proposed a new method of inner surface modification by PSII. We used a coaxial central pole and a grounded cylindrical grid electrode in a tube sample, and the system is called the grid-enhanced plasma source ion implantation (GEPSII). The system can resolve two difficulties at the same time [8, 9].

Because ions move mostly in line in electric field, the grounded grid lines can block the ions paths when they diffuse from the grid electrode inner to the outside and then the grid shadow can be seen on the sample coating surfaces. This will affect the application of the GEPSII for inner surface modification. In our previous research, protective TiN films on the 45# steel sample surfaces in thickness of tens of nanometer can greatly improve the anticorrosion ability of 45#steel. At the same time we found the grid shadow effects on the 45# steel surfaces after their electrochemistry corrosion tests. Therefore, We systematically implanted TiN films on crystal silicon sample surfaces and checked their surface topography to see the detailed difference between the shadow area and un-shadow area.

2. Concept of GEPSII Inner Surface Modification

Figure 1 schematically shows our GEPSII experimental set-up for inner surface modification of a cylindrical tube. The system consists mainly of two titanium (Ti) coaxial electrodes, the central axial electrode and the coaxial-earthed grid electrode. N_2 plasma can be produced between them by a 13.56 MHz rf oscillation. The tube was really the cylinder of an automobile with a diameter of 100 mm and a length of 210-mm; the cylindrical grid electrode, made of stainless steel net with the mesh of a size 0.9 mm×0.9 mm, had a diameter of 48 mm and a length of 230 mm. For the convenience of experimental detection, we placed several 45# steel samples and single-crystal silicon samples on the inner surface bottom side of the tube along the axial direction.

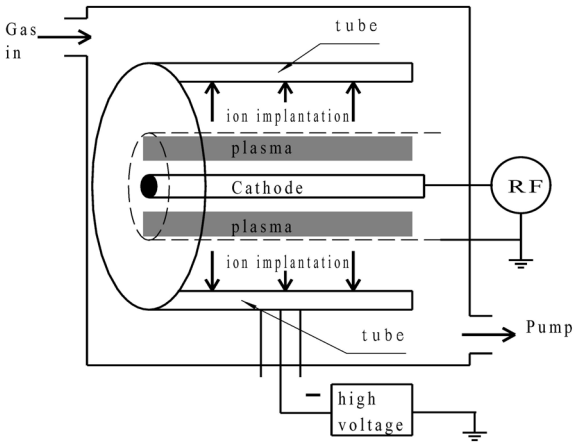

Fig. 1. Illustration of GEPSII experimental system

The electrochemical corrosion tests were carried out on a M351 potentiometer, which gave the testing

Tafel curves. And the corrosion tests was done in 2% NaCl solution. The surface topography of the TiN films on silicon surface was investigated by using an atomic force microscope (NanoScope IIIa/AFM).

3. Results and Discussions

Electrochemical corrosion test give the Log (I)-V polarization curves called Tafel curves. We can obtain pitting corrosion potential (E_{corr}) and corrosion rates from the Tafel curves. The pitting corrosion potential is obtained at the beginning of the test and given as the start of the voltage axis; and the corrosion rates are represented by the free corrosion current (I_k). The electrochemistry parameters of the processed samples are shown in Fig. 2. Nitrogen pressure is 10 Pa, rf power is 150 W and pulsed voltage is –10 kV, 60 Hz, direct current voltage is –2 kV. The value of E_{corr} stands for the resistance ability against the pitting corrosion, the sample with a higher E_{corr} has relatively higher corrosion resistance. The passivating phenomenon in the curves in Fig. 2 shows that the coated films work well. Here the passivated film is different from the produced film of steel passivated by itself in strong acid, and the refers to the coated TiN films. For passivating curves the current value at the passivating inflection point is the I_k of the film, and for the curve without passivating phenomenon, it is the current value at the intersection point of x-axis and the tangent of the curve at about 100 mV above the E_{corr}. The lower I_k means the lower corrosion rate, and thus means a higher anticorrosion ability. E_{corr} and I_k given in Fig. 2 indicate that all coated films have higher corrosion resistance than the uncoated sample does. The dc-implanted film, with $E_{corr} = -8$mV and $I_k =$ $= 1.5\times10^{-8}$A/cm^2, is several hundreds times improved.

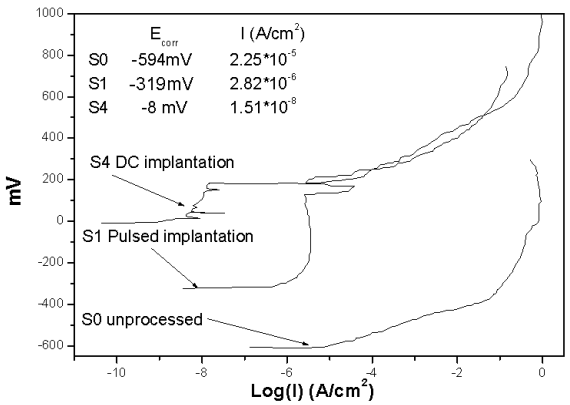

Fig. 2. Tafel curves of different voltages of implanted coatings (anode reactive)

And the pulsed negative high-voltage implanted film, with $E_{corr} = -319$ mV and $I_k = 2.82\cdot10^{-6}$ A/cm^2, is about 10 times improved. Because the total injection current of the dc implantation is larger than that of the pulsed implantation, the dc-implanted film has a higher corrosion resistance than the pulsed implanted film does. In anodic reaction, iron atoms lose electrons and dissolve into the salt solution. The coated film protects the 45# steel substrate with a dense microstructure from corrosion reactions.

The protective TiN films on the 45# steel sample surfaces can greatly improve the anticorrosion ability of 45#steel. But, at the same time we found the grid shadow effects on the 45# steel surfaces after their electrochemistry corrosion tests. Therefore, We systematically implanted TiN films on crystal silicon sample surfaces and checked their surface topography to see the detailed difference between the shadow area and the un-shadow area.

Figures 3, a and b show different areas on one implanted sample, which is obtained at 0.1 Pa nitrogen pressure, 15 kV pulsed negative voltage and 24 mm grid electrode radius. Fig. 3, a exhibits the AFM topography of the shadow area and Fig. 3, b shows the AFM topography of the un-shadow area on the same sample surface. From Fig. 3, a we can see 10~30 nm sized bulk TiN grains randomly and loosely arranged on silicon surface, while in Fig. 3, b the grains grow much tighter than those in Fig. 3, a. Surely the surface characteristics of these two areas are different, and this difference can induce a grid shadow on the corrosion tested 45# steel sample surfaces. In corrosion tests, the shadow area will be firstly etched off and then the protective film will lose its function.

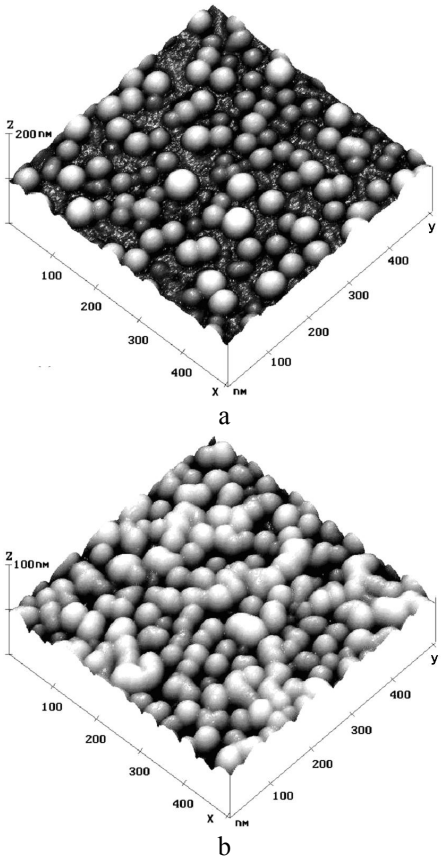

Fig. 3. Surface topography by AFM in the different area of one sample obtained at the nitrogen pressure of 0.1 Pa, the pulsed negative voltage of 15 kV and 24 mm the grid electrode radius, shadow area (a), un-shadow area (b)

It is found that when the discharge nitrogen gas pressure is lower than 1 Pa and the implanting voltage is higher than 20 kV, we may see the clear grid shadow on the sample surfaces directly. If we increase the gas pressure or reduce the implanting voltage, the shadow effect will be weakened. Figs. 4, a and b show different areas on another implanted sample obtained at 5-Pa nitrogen pressure, 10-kV pulsed negative voltage and 24-mm grid electrode radius. Fig. 4, a shows the AFM topography of the shadow area and Fig. 4, b illustrates the AFM topography of the un-shadow area. The film in Fig. 4, a is thinner than the film in Fig. 4, b and we can see that the grains in Fig. 3(b) grow tighter than those in Fig. 4, b; it is because the higher implanting voltage will lead to the higher grown stress.

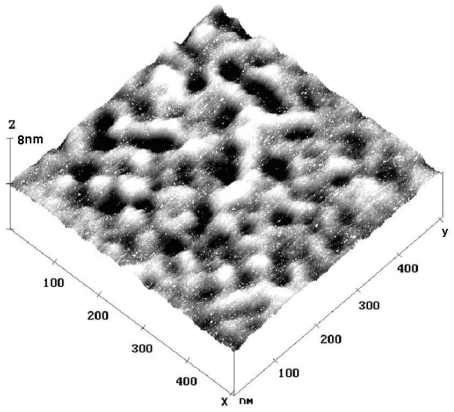

a

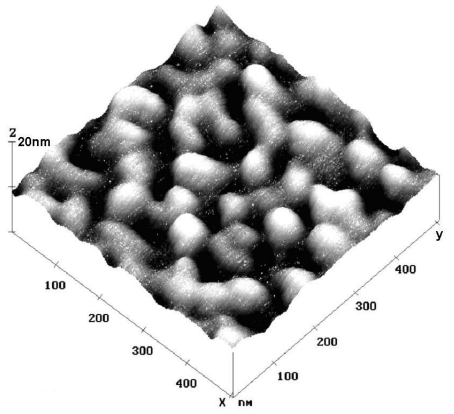

b

Fig. 4. Surface topography by AFM in the different area of one sample obtained at the Nitrogen pressure of 5Pa, the pulsed negative voltage of 10 kV and 24 mm the grid electrode radius, shadow area (a), un-shadow area (b)

By continuously changing the discharge conditions, it is found that the shadow effect directly relates to gas pressure and implanted voltage. Higher gas pressure and lower pulsed voltage can reduce the shadow effect. At the experimental conditions of 100 Pa nitrogen pressure and 2 kV direct current implanting voltage, the surface shadow effect almost disappears. Its surface anti-corrosion ability is much better than that when we use the pulsed high voltage. Furthermore, the shadow effect also relates to the radius of grid electrode, i.e., the gap distance between grid electrode and tube inner surface. In our experiments we used two radii, 24 mm and 38 mm, the experimental results show that larger radius can enhance the shadow effect.

As is known, ions can absolutely move in line in electric field if there are not particle collisions. Since the grid lattice will block the moving path of some ions, there will be some areas of the sample surface nearly without or with few ions arriving, which will form the shadow area. We know that ions diffusing from the grid will collide with nitrogen molecules outside the grid, and the collision will make ions deviate from their original moving path, which will reduce the shadow effect. The number of collisions of an ion suffered before implantation will determine the extent of ion deviation from its original moving path. Since higher pressure and longer moving distance will raise the rate of ion collisions, the shadow effect will be weakened accordingly. However, we know that too much collision will reduce the implanting energy of ions [10]. At higher implanting voltage, ions will move with higher energy and reach target with a smaller drift rate, this will enhance the shadow effect. While the smaller implanting voltage will lead to the smaller surface film growing stress and the implanted depth, and then the surface mechanical performance will be reduced.

So it is not a good idea to weaken the shadow effect by using low implanting voltage, because low implanting voltage will reduce the implanted effect. To settle this problem, we used an axial magnetic field along the tube by winding coil on the tube ectotheca. Cylindrical plasma in axial magnetic field will produce circumference momentum current [11], will change the electron track and increase the rate of electron colliding with neutral molecules, and so will increase the plasma-ionized rate. Then the plasma density inside the tube will be increased and mixed.

Figure 5 shows the optical intensity of magnetic plasma and non-magnetic plasma measured by scattering optical spectrometer. We can use optical intensity describing plasma density in the tube. In Fig. 5, the plasma density outside the grid is increased by the axial magnetic field and the plasma is mixed. Therefore, the shadow effect of the sample surfaces will be weakened. In our experiments, magnetic induction is 50 Gauss, and after the magnetic GEPSII processing, the sample surface became cleaner than that without the magnetic GEPSII and the shadow effect was weakened too.

Figure 6 presents the AFM topography of the magnetic GEPSII processed sample surface obtained at 5 Pa nitrogen pressure, 10 kV pulsed negative voltage and 24 mm grid electrode radius. At the sample surface we have not found the shadow effect with an AFM, and the TiN grains are bigger and tighter than those in Fig. 4, b. When the magnetic GEPSII proc-

essing conditions are changed into 0.1 Pa nitrogen pressure, 15 kV pulsed negative voltage and 24 mm grid electrode radius, we can see the shadow effect but it is weaker than that without magnetic field.

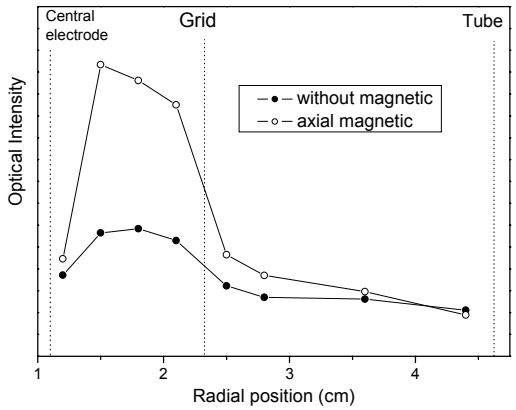

Fig. 5. Radial optical intensity distribution of magnetic plasma and non-magnetic plasma measured by scattering optical spectrometer

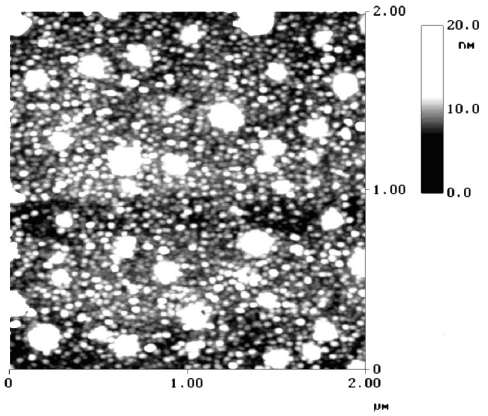

Fig. 6. AFM topography of magnetic GEPSII processed sample surface obtained at 5-Pa Nitrogen pressure, 10-kV pulsed negative voltage and 24-mm grid electrode radius

4. Conclusion

In conclusion, we have studied the anti-corrosion effect of GEPSII processed 45#steel sample and the grid shadow effect. The shadow effect is due to the fact that ions move mostly in line in electric filed and the grid lines block their paths. High gas pressure, small grid radius and low implanting voltage can weaken the shadow effect. A 50-Gauss axial magnetic field can increase the plasma density and weaken the shadow effect by mixing the plasma outside the grid in our experiments

Acknowledgement

This work was Supported by the National High Technology Research and Development Program of China (Grant No. 2002A331020), the National Natural Science Foundation of China (Grant Nos. 50071068 and 10275088), the Science and Technology Program of Beijing Municipal Science and Technology Commission (Grant No. H020420160130), and the ARO-FE of USA (Grant No. N62649-02-1-0010)

References

[1] J. Chen, J. Blanchard, J.R. Conrad, and R.A. Dodd, Surf. Coat. Technol. **53**, 267 (1992).
[2] J.V. Mantese, I.G. Brown, N.W. Cheung, and G.A. Collins, MRS Bull. **21,** 52 (1996).
[3] W. Ensinger, Rev. Sci. Instrum. **67,** 318 (1996).
[4] O. Demokan, IEEE Transactions on Plasma Science. **28,** 1720 (2000).
[5] S. Shinji, Thin Solid Film **316,** 165 (1998).
[6] S. Sugimoto, Y. Uchikawa, K. Kuwahara, and H. Kuwahara, Jpn. J. Appl. Phys. **38,** 4342 (1999).
[7] M. Sun, C.Z. Liu and S.Z. Yang, J. Vac. Sci. Technol. A **14,** 367 (1996).
[8] B. Liu, G.L. Zhang, and S.Z. Yang, J. Vac. Sci. Technol. *A* **19,** 295 (2001).
[9] G.L. Zhang, J.L. Wang, and S.Z. Yang, Acta Phys. Sin. **52,** 2213 (2003) (in Chinese).
[10] J.L. Wang, G.L. Zhang, S.H. Fan, and S.Z. Yang, J. Phys D: Appl Phys **36,** 1192 (2003).
[11] F.F. Chen, *Introduction to Plasma Physics and Controlled Fusion, second edition, vol. 1: Plasma Physics* (New York, Plenum Press), 1984, pp. 69–70.